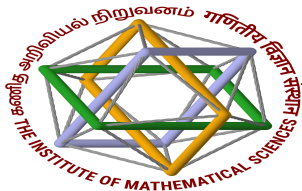


The QCD Equation of state at finite density from lattice

Sayantana Sharma



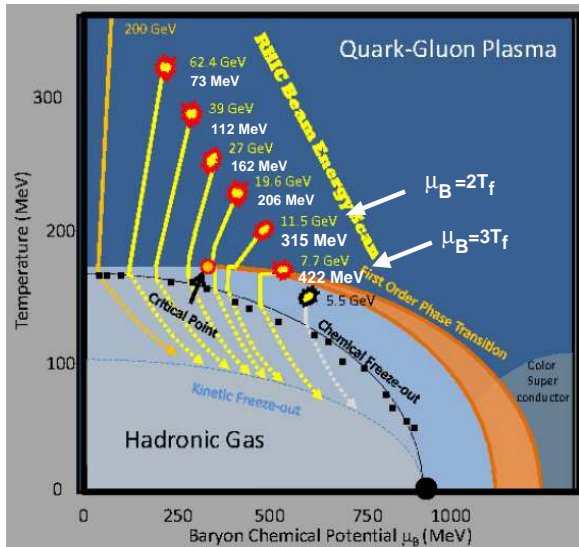
December 11, 2018

Outline

- 1 The QCD phase diagram: outstanding issues from lattice QCD
- 2 Equation of state at finite μ_B
- 3 Critical-end point search from lattice

- 1 The QCD phase diagram: outstanding issues from lattice QCD
- 2 Equation of state at finite μ_B
- 3 Critical-end point search from lattice

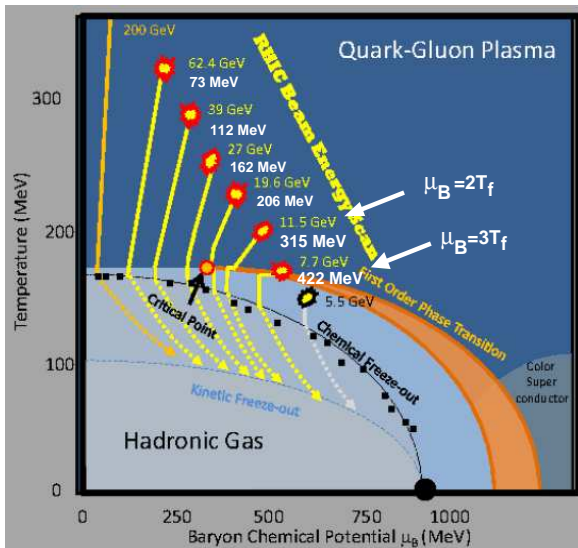
Perspectives from Lattice QCD



[<http://www.bnl.gov/rhic/news>]

Perspectives from Lattice QCD

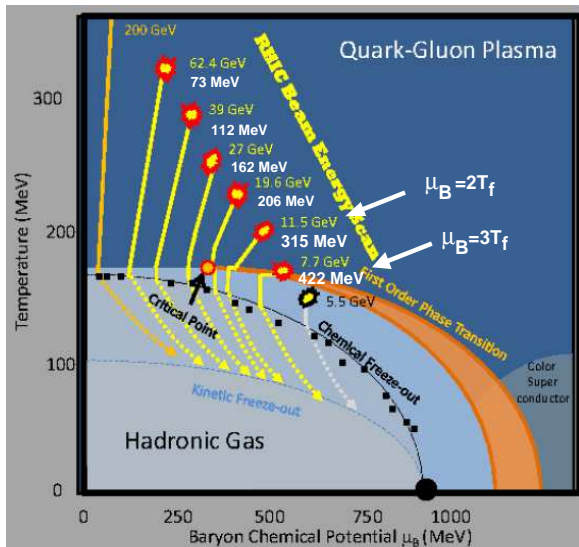
- In view of the RHIC Beam Energy Scan-II in 2019-20 $\mu_B/T \leq 3$ it is important to have control over the Equation of State for $\mu_B/T \leq 3$.



[<http://www.bnl.gov/rhic/news>]

Perspectives from Lattice QCD

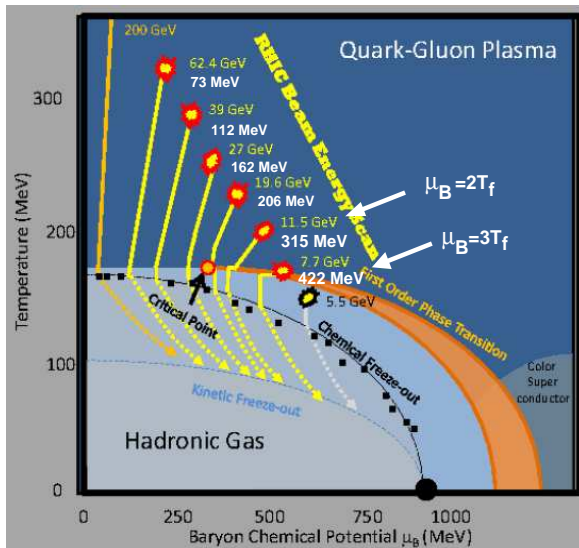
- In view of the RHIC Beam Energy Scan-II in 2019-20 $\mu_B/T \leq 3$ it is important to have control over the Equation of State for $\mu_B/T \leq 3$.
- Measure the curvature of chiral and freezeout curves expected from QCD thermodynamics.



[<http://www.bnl.gov/rhic/news>]

Perspectives from Lattice QCD

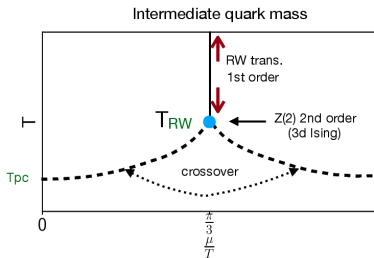
- In view of the RHIC Beam Energy Scan-II in 2019-20 baryon chemical potential scan it is important to have control over the Equation of State for $\mu_B/T \leq 3$.
- Measure the curvature of chiral and freezeout curves expected from QCD thermodynamics.
- Look for possible existence and bracket the position of **critical end-point** in the phase diagram.



[<http://www.bnl.gov/rhic/news>]

Lattice techniques at finite μ_B -I

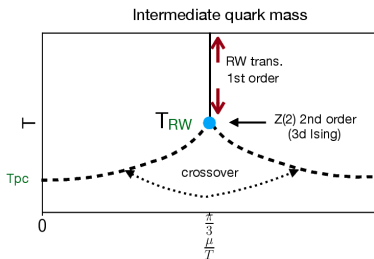
- Conventional Monte-Carlo methods suffer from **sign problem** at finite μ_q .
- Two methods presently allow to go to thermodynamic and continuum limits.



[From arXiv:1811.02494]

Lattice techniques at finite μ_B -I

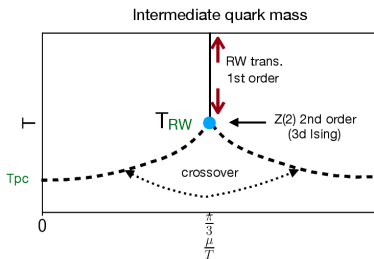
- Conventional Monte-Carlo methods suffer from **sign problem** at finite μ_q .
- Two methods presently allow to go to thermodynamic and continuum limits.
- For **imaginary μ_q** the fermion determinant real and positive \rightarrow no sign-problem.



[From arXiv:1811.02494]

Lattice techniques at finite μ_B -I

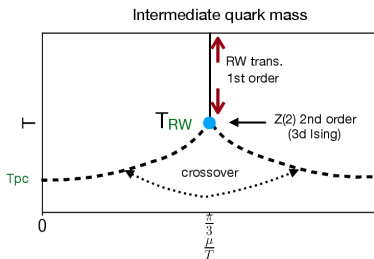
- Conventional Monte-Carlo methods suffer from **sign problem** at finite μ_q .
- Two methods presently allow to go to thermodynamic and continuum limits.
- For **imaginary** μ_q the fermion determinant real and positive \rightarrow no sign-problem.
- $\mathcal{Z}_{QCD}(\mu_q/T) = \mathcal{Z}_{QCD}(\mu_q/T + 2ni\pi/3)$ implies Roberge-Weiss end-points at $\mu_q/T = (2n+1)i\pi/3$.



[From arXiv:1811.02494]

Lattice techniques at finite μ_B -I

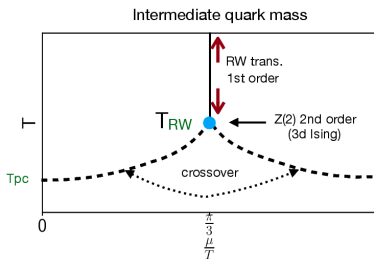
- Conventional Monte-Carlo methods suffer from **sign problem** at finite μ_q .
- Two methods presently allow to go to thermodynamic and continuum limits.
- For **imaginary** μ_q the fermion determinant real and positive \rightarrow no sign-problem.
- $\mathcal{Z}_{QCD}(\mu_q/T) = \mathcal{Z}_{QCD}(\mu_q/T + 2ni\pi/3)$ implies Roberge-Weiss end-points at $\mu_q/T = (2n+1)i\pi/3$.
- Calculate baryon no. density at several $\mu_q/T < i\pi/3$.



[From arXiv:1811.02494]

Lattice techniques at finite μ_B -I

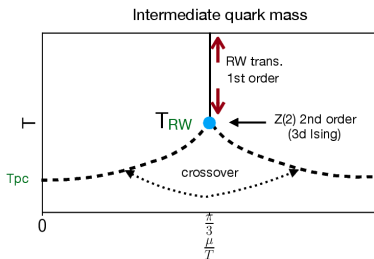
- Conventional Monte-Carlo methods suffer from **sign problem** at finite μ_q .
- Two methods presently allow to go to thermodynamic and continuum limits.
- For **imaginary** μ_q the fermion determinant real and positive \rightarrow no sign-problem.
- $\mathcal{Z}_{QCD}(\mu_q/T) = \mathcal{Z}_{QCD}(\mu_q/T + 2ni\pi/3)$ implies Roberge-Weiss end-points at $\mu_q/T = (2n+1)i\pi/3$.
- Calculate baryon no. density at several $\mu_q/T < i\pi/3$.
- Fitting it to a polynomial in μ_q analytically continue in the real- μ plane.



[From arXiv:1811.02494]

Lattice techniques at finite μ_B -I

- Conventional Monte-Carlo methods suffer from **sign problem** at finite μ_q .
- **Two methods presently allow to go to thermodynamic and continuum limits.**
- For **imaginary μ_q** the fermion determinant real and positive \rightarrow no sign-problem.
- $\mathcal{Z}_{QCD}(\mu_q/T) = \mathcal{Z}_{QCD}(\mu_q/T + 2ni\pi/3)$ implies Roberge-Weiss end-points at $\mu_q/T = (2n+1)i\pi/3$.
- Calculate baryon no. density at several $\mu_q/T < i\pi/3$.
- Fitting it to a polynomial in μ_q analytically continue in the real- μ plane.
- **Limited due to discontinuities at Roberge-Weiss end-points!**



[From arXiv:1811.02494]

Lattice techniques at finite μ_B -II

- **Taylor expansion** of physical observables around $\mu = 0$ in powers of μ/T [Bi-Swansea collaboration, 02]

$$\frac{P(\mu_B, T)}{T^4} = \frac{P(0, T)}{T^4} + \left(\frac{\mu_B}{T}\right)^2 \underbrace{\frac{\chi_2^B(0, T)}{2T^2}}_{P_2} + \left(\frac{\mu_B}{T}\right)^4 \frac{\chi_4^B(0)}{4!} + \dots$$

P_4

- The series for $\chi_2^B(\mu_B)$ should diverge at the critical point. On finite lattice χ_2^B peaks, ratios of Taylor coefficients equal, indep. of volume [Gavai & Gupta, 03]

Challenges for Taylor expansion

- The fluctuations of conserved charges can be expressed in terms of Quark no. susceptibilities (QNS).

Challenges for Taylor expansion

- The fluctuations of conserved charges can be expressed in terms of Quark no. susceptibilities (QNS).
- QNS χ_{ij} 's can be written as derivatives of the Dirac operator.

Example: $\chi_2^u = \frac{T}{V} \langle \text{Tr}(D_u^{-1} D_u'' - (D_u^{-1} D_u')^2) + (\text{Tr}(D_u^{-1} D_u'))^2 \rangle.$

$\chi_{11}^{us} = \frac{T}{V} \langle \text{Tr}(D_u^{-1} D_u' D_s^{-1} D_s') \rangle.$

Challenges for Taylor expansion

- The fluctuations of conserved charges can be expressed in terms of Quark no. susceptibilities (QNS).
- QNS χ_{ij} 's can be written as derivatives of the Dirac operator.

$$\text{Example: } \chi_2^u = \frac{T}{V} \langle \text{Tr}(D_u^{-1} D_u'' - (D_u^{-1} D_u')^2) + (\text{Tr}(D_u^{-1} D_u'))^2 \rangle.$$

$$\chi_{11}^{us} = \frac{T}{V} \langle \text{Tr}(D_u^{-1} D_u' D_s^{-1} D_s') \rangle.$$

- Higher derivatives \rightarrow more inversions
Inversion is the most expensive step on the lattice !

Challenges for Taylor expansion

- The fluctuations of conserved charges can be expressed in terms of Quark no. susceptibilities (QNS).
- QNS χ_{ij} 's can be written as derivatives of the Dirac operator.

$$\text{Example: } \chi_2^u = \frac{T}{V} \langle \text{Tr}(D_u^{-1} D_u'' - (D_u^{-1} D_u')^2) + (\text{Tr}(D_u^{-1} D_u'))^2 \rangle.$$

$$\chi_{11}^{us} = \frac{T}{V} \langle \text{Tr}(D_u^{-1} D_u' D_s^{-1} D_s') \rangle.$$

- Higher derivatives \rightarrow more inversions
Inversion is the most expensive step on the lattice !
- Why extending to higher orders so difficult?

Challenges for Taylor expansion

- The fluctuations of conserved charges can be expressed in terms of Quark no. susceptibilities (QNS).
- QNS χ_{ij} 's can be written as derivatives of the Dirac operator.

$$\text{Example: } \chi_2^u = \frac{T}{V} \langle \text{Tr}(D_u^{-1} D_u'' - (D_u^{-1} D_u')^2) + (\text{Tr}(D_u^{-1} D_u'))^2 \rangle.$$

$$\chi_{11}^{us} = \frac{T}{V} \langle \text{Tr}(D_u^{-1} D_u' D_s^{-1} D_s') \rangle.$$

- Higher derivatives \rightarrow more inversions
Inversion is the most expensive step on the lattice !
- Why extending to higher orders so difficult?
 - Matrix inversions increasing with the order

Challenges for Taylor expansion

- The fluctuations of conserved charges can be expressed in terms of Quark no. susceptibilities (QNS).

- QNS χ_{ij} 's can be written as derivatives of the Dirac operator.

$$\text{Example: } \chi_2^u = \frac{T}{V} \langle \text{Tr}(D_u^{-1} D_u'' - (D_u^{-1} D_u')^2) + (\text{Tr}(D_u^{-1} D_u'))^2 \rangle.$$

$$\chi_{11}^{us} = \frac{T}{V} \langle \text{Tr}(D_u^{-1} D_u' D_s^{-1} D_s') \rangle.$$

- Higher derivatives \rightarrow more inversions

Inversion is the most expensive step on the lattice !

- Why extending to higher orders so difficult?
 - Matrix inversions increasing with the order
 - Delicate cancellation between a large number of terms for higher order QNS.

Recent developments: A new method to introduce μ

- The staggered fermion matrix used at finite μ [Hasenfratz, Karsch, 83]

$$D(\mu)_{xy} = \sum_{i=1}^3 \eta_i(x) \left[U_i^\dagger(y) \delta_{x,y+\hat{i}} - U_i(x) \delta_{x,y-\hat{i}} \right] \\ + \eta_4(x) \left[e^{\mu a} U_4^\dagger(y) \delta_{x,y+\hat{4}} - e^{-\mu a} U_4(x) \delta_{x,y-\hat{4}} \right]$$

Recent developments: A new method to introduce μ

- The staggered fermion matrix used at finite μ [Hasenfratz, Karsch, 83]

$$D(\mu)_{xy} = \sum_{i=1}^3 \eta_i(x) \left[U_i^\dagger(y) \delta_{x,y+\hat{i}} - U_i(x) \delta_{x,y-\hat{i}} \right] \\ + \eta_4(x) \left[e^{\mu a} U_4^\dagger(y) \delta_{x,y+\hat{4}} - e^{-\mu a} U_4(x) \delta_{x,y-\hat{4}} \right]$$

- One can also add μ coupled to the conserved number density as in the continuum.

$$D(0)_{xy} - \frac{\mu a}{2} \eta_4(x) \left[U_4^\dagger(y) \delta_{x,y+\hat{4}} + U_4(x) \delta_{x,y-\hat{4}} \right].$$

Pros and Cons

- Linear method: $D' = \sum_{x,y} N(x,y)$, and
 $D'' = D''' = D'''' \dots = 0$

in contrast to the Exp-prescription, all derivatives are non-zero.

Pros and Cons

- Linear method: $D' = \sum_{x,y} N(x,y)$, and
 $D'' = D''' = D'''' \dots = 0$

in contrast to the Exp-prescription, all derivatives are non-zero.

- No. of inversions significantly reduced for higher orders in linear method.

For 8th order QNS the no. of matrix inversions reduced from 20 to 8 for staggered fermions. [Gavai & Sharma, 12]

Pros and Cons

- Linear method: $D' = \sum_{x,y} N(x,y)$, and
 $D'' = D''' = D'''' \dots = 0$

in contrast to the Exp-prescription, all derivatives are non-zero.

- No. of inversions significantly reduced for higher orders in linear method.

For 8th order QNS the no. of matrix inversions reduced from 20 to 8 for staggered fermions. [Gavai & Sharma, 12]

- Linear method: χ_n have additional zero- T artifacts. \rightarrow explicit counter terms needed for $\chi_{2,4}$, discussed in detail [Gavai & Sharma, 15]

Pros and Cons

- Linear method: $D' = \sum_{x,y} N(x,y)$, and
 $D'' = D''' = D'''' \dots = 0$

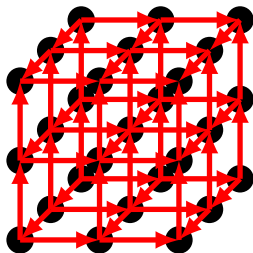
in contrast to the Exp-prescription, all derivatives are non-zero.

- No. of inversions significantly reduced for higher orders in linear method.

For 8th order QNS the no. of matrix inversions reduced from 20 to 8 for staggered fermions. [Gavai & Sharma, 12]

- Linear method: χ_n have additional zero- T artifacts. \rightarrow explicit counter terms needed for $\chi_{2,4}$, discussed in detail [Gavai & Sharma, 15]
- In Exp method: counter terms already at the Lagrangian level. We use this method for χ_n^B , $n = 2, 4$.

Our Set-up



- $V = N^3 a^3$, Box size: $m_\pi V^{1/3} > 4$.
- $T = \frac{1}{N_\tau a}$
We use $N_\tau = 6, 8, 12, 16$ lattices for $\chi_{2,4}$ and $N_\tau = 6, 8$ for higher order fluctuations.
- Input m_s physical and $m_\pi^G = 160$ MeV for $T > 175$ MeV and $m_\pi^G = 140$ MeV for $T \leq 175$ MeV.

Outline

- 1 The QCD phase diagram: outstanding issues from lattice QCD
- 2 Equation of state at finite μ_B
- 3 Critical-end point search from lattice

EoS in the constrained case

- In most central heavy-ion experiments typically:

$n_S = 0$, **Strangeness neutrality**,

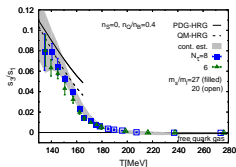
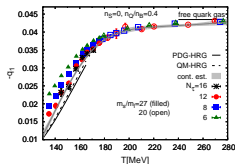
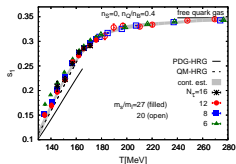
$$\frac{n_Q}{n_B} = \frac{n_P}{n_P + n_N} = 0.4.$$

[Bi-BNL collaboration, 1208.1220]

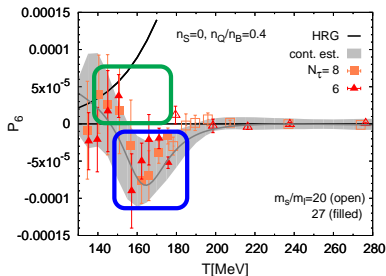
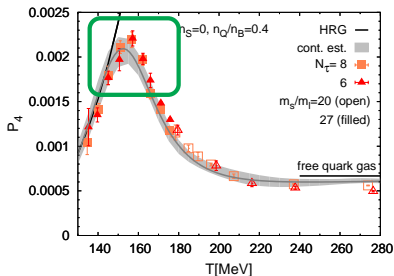
- For lower \sqrt{s} collisions: **Need to understand baryon stopping!**
- Imposes non-trivial constraints on the variation of μ_S and μ_Q .
- Possible to vary them by only varying μ_B through

$$\mu_S = s_1 \mu_B + s_3 \mu_B^3 + s_5 \mu_B^5 + \dots$$

$$\mu_Q = q_1 \mu_B + q_3 \mu_B^3 + q_5 \mu_B^5 + \dots$$

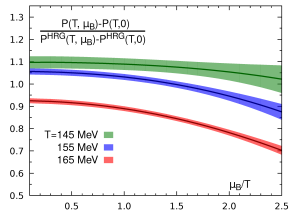
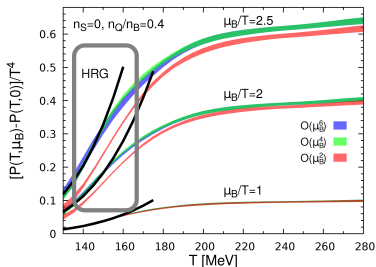


- Central values of P_4, P_6 already deviate from Hadron Resonance gas model at $T > 145$ MeV \rightarrow need to analyze the errors on P_6 better.
- P_6 has characteristic structure at $T > T_c \rightarrow$ remnant of the chiral symmetry due to the light quarks. Effects of $U_A(1)$ anomaly?
- Essentially non-perturbative \rightarrow cannot be predicted within Hard Thermal Loop perturbation theory.



EoS in the constrained case

- The EoS is well under control for $\mu_B/T \sim 2.5$ with χ_6 .
- Full parametric dependence for N_B on T available in [arxiv: 1701.04325](https://arxiv.org/abs/1701.04325).
- Expanding to $\mu_B/T = 3$, need to calculate χ_8 !

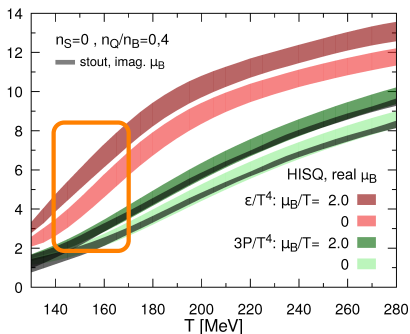


Summary for the EoS

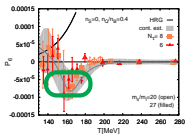
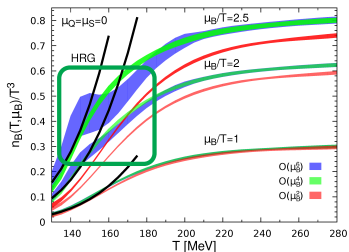
- Continuum estimates from two different fermion discretization agree for $\mu_B/T \leq 2$.

[Bielefeld-BNL-CCNU collaboration, 1701.04325, Borsanyi et. al, 1606.07494].

- Steeper EoS for RHIC energies compared to LHC energy.



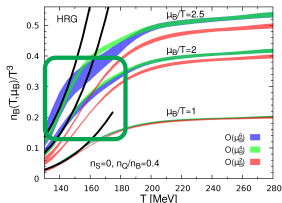
Baryon number density



- χ_6 contribution is 30-times larger than in pressure.

$$\frac{N(\mu_B)}{T^3} = \frac{\mu_B}{T} \chi_2^B(0) + \frac{1}{2} \left(\frac{\mu_B}{T} \right)^4 \chi_4^B(0) + \frac{1}{4!} \left(\frac{\mu_B}{T} \right)^6 \chi_6^B(0) + \dots$$

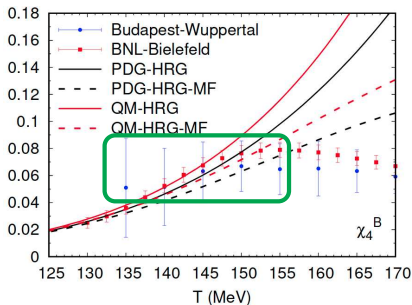
- Strongly sensitive to the singular part of χ_6^B .



- For strangeness neutral system, effect is milder.

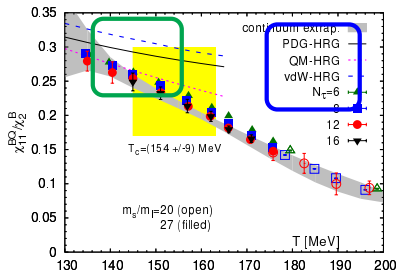
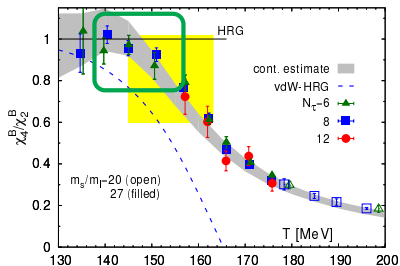
Can $T < T_c$ be described by Hadron Resonance Gas?

- Effects of interactions between hadrons can be mimicked by free gas of **resonances+hadrons?**
- Some baryon channels do not have resonances. **In-medium modification of baryons?**
- Lattice data for higher order baryon no. fluc. are precise enough to distinguish between diff. scenarios \rightarrow **support additional resonances from quark-models+interactions**



[P. Huovinen, P. Petreczky, 1811.09330]

Can $T < T_c$ be described by Hadron Resonance Gas?



[F. Karsch, QM17 proceedings, 1706.01620]

- Including Van der Waal's interaction for baryons+non-interacting mesons+resonances, new versions of HRG has been studied \rightarrow significant deviation from non-interacting HRG.

[V. Vovchenko, M. I. Gorenstein and H. Stoecker 1609.03975]

- Lattice data can constrain such models strongly! Currently none of these models are perfect to describe QCD at freezeout.

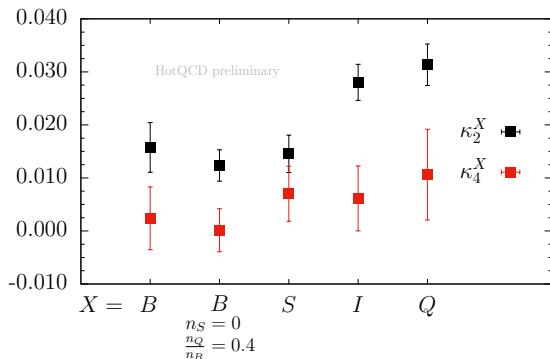
Outline

- 1 The QCD phase diagram: outstanding issues from lattice QCD
- 2 Equation of state at finite μ_B
- 3 Critical-end point search from lattice

Curvature of the chiral crossover line

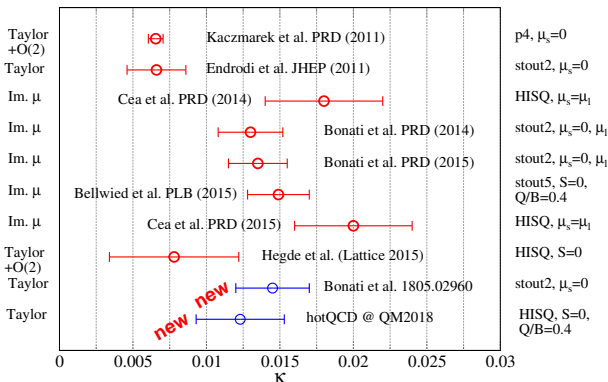
- $\frac{T_c(\mu_X)}{T_c(0)} = 1 - \kappa_2^X \frac{\mu_X^2}{T_c(0)^2} - \kappa_4^X \frac{\mu_X^4}{T_c(0)^4}$
- For strangeness neutral system, continuum results available!
 $\kappa_2^B = 0.012(4)$, $\kappa_4^B \sim 0$ with Taylor expansions and HISQ fermions.

[HotQCD collaboration, 1807.05607, and in prep.]



Curvature of the chiral crossover line

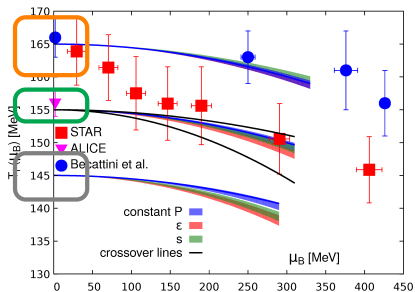
- $\frac{T_c(\mu_X)}{T_c(0)} = 1 - \kappa_2^X \frac{\mu_X^2}{T_c(0)^2} - \kappa_4^X \frac{\mu_X^4}{T_c(0)^4}$
- Consistent with imaginary chemical potential method and stout fermions
 $\kappa_2^B = 0.0135(20)$ [C. Bonati et. al., 1805.02960]
- removes earlier tension between two methods! [courtesy M. D'Elia Quark Matter 18]



Curvature of freeze-out line vs chiral crossover line

- Different LCP's agree within 2 MeV for $\mu_B/T \leq 2$ for 3 initial choices of T_0 .
- For lines $P = \text{const}$, the entropy density changes by 15% \rightarrow better description of LCP for viscous medium formed in heavy-ion collisions.

[HotQCD collaboration, 1701.04325].



- STAR results give a steeper curvature. [arXiv:1412.0499].
- Agreement with the recent ALICE results. [arXiv:1408.6403].
- Consistent with phenomenological models. [Becattini et. al., 1605.09694].

Critical-end point search from Lattice

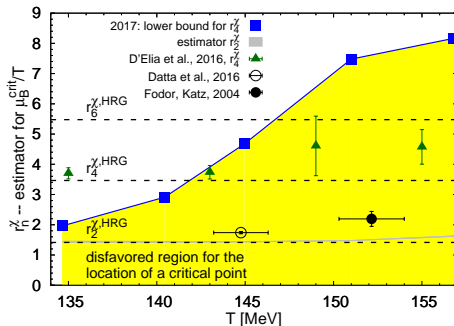
- The Taylor series for $\chi_2^B(\mu_B)$ should diverge at the critical point. On finite lattice χ_2^B peaks, ratios of Taylor coefficients equal, indep. of volume.
- The radius of convergence determines location of the critical point.

[Gavai & Gupta, 03]

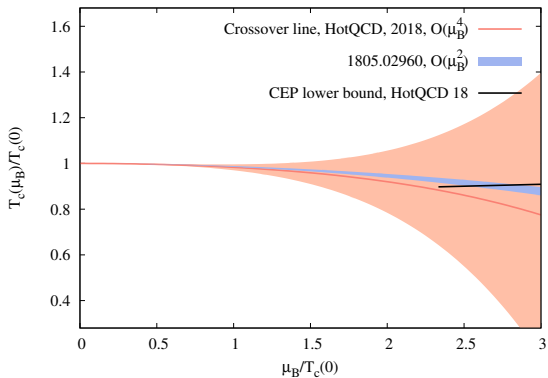
- Definition: $r_{2n} \equiv \sqrt{2n(2n-1) \left| \frac{\chi_{2n}^B}{\chi_{2n+2}^B} \right|}$.
 - Strictly defined for $n \rightarrow \infty$. **How large n could be on a finite lattice?**
 - Signal to noise ratio deteriorates for higher order χ_n^B .

Critical-end point search from Lattice

- Current bound for CEP: $\mu_B/T > 3$ for $142 \leq T \leq 150$ MeV
[HotQCD coll., 1701.04325, update 2018].
- The r_n extracted by analytic continuation of imaginary μ_B data
[D'Elia et. al., 1611.08285] consistent with this bound.
- Results with a lower bound? [Datta et. al., 1612.06673, Fodor and Katz, 04] \rightarrow need to understand the systematics in these studies. Ultimately all estimates will agree in the continuum limit!

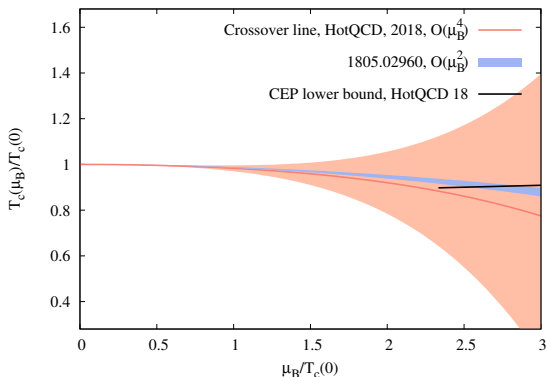


Critical end-point and Chiral Crossover line: current status



Steeper curvature would imply slow convergence of r_n with order n

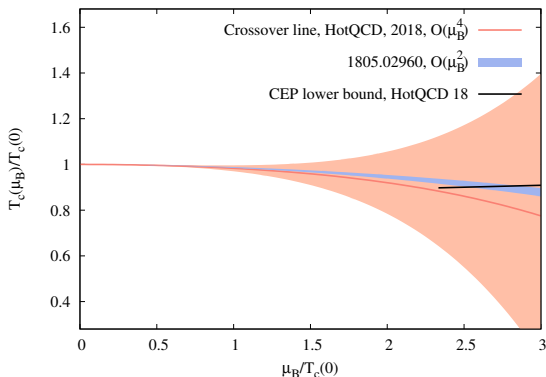
Critical end-point and Chiral Crossover line: current status



- For current trends
 $\kappa_4 = \kappa_6 = \kappa_8 \dots \sim 0$,
radius of curvature
estimates tell us
 $T_{CEP} \sim 0.92 T_c(0)$ and
 $\mu_B/T_{CEP} > 3$.

Steeper curvature would imply slow convergence of r_n with order n

Critical end-point and Chiral Crossover line: current status



- For current trends $\kappa_4 = \kappa_6 = \kappa_8 \dots \sim 0$, radius of curvature estimates tell us $T_{CEP} \sim 0.92 T_c(0)$ and $\mu_B/T_{CEP} > 3$.
- If $\kappa_4 \sim 0.1\kappa_2$, only significantly contributes when $\mu_B/T_{CEP} > 3$ so its precise determination is imp.

Steeper curvature would imply slow convergence of r_n with order n

Outlook

- Preparing for BES-II runs: LQCD EoS important for hydrodynamic modeling of QGP. For $\mu_B/T \leq 2 \rightarrow \sqrt{s_{NN}} \geq 11$ GeV already under control with χ_6^B .

Outlook

- Preparing for BES-II runs: LQCD EoS important for hydrodynamic modeling of QGP. For $\mu_B/T \leq 2 \rightarrow \sqrt{s_{NN}} \geq 11$ GeV already under control with χ_6^B .
- χ_8^B is important to estimate the errors on the EoS measured with the sixth order cumulants and going towards $\mu_B/T = 3$.

Outlook

- Preparing for BES-II runs: LQCD EoS important for hydrodynamic modeling of QGP. For $\mu_B/T \leq 2 \rightarrow \sqrt{s_{NN}} \geq 11$ GeV already under control with χ_6^B .
- χ_8^B is important to estimate the errors on the EoS measured with the sixth order cumulants and going towards $\mu_B/T = 3$.
- Lines of constant ϵ, p consistent with LQCD estimates of curvature of chiral crossover line.

Outlook

- Preparing for BES-II runs: LQCD EoS important for hydrodynamic modeling of QGP. For $\mu_B/T \leq 2 \rightarrow \sqrt{s_{NN}} \geq 11$ GeV already under control with χ_6^B .
- χ_8^B is important to estimate the errors on the EoS measured with the sixth order cumulants and going towards $\mu_B/T = 3$.
- Lines of constant ϵ, p consistent with LQCD estimates of curvature of chiral crossover line.
- Higher order cumulants of baryon no. will also help in bracketing the possible CEP. Most LQCD calculations suggest $\mu_B(\text{CEP})/T \geq 3$.